

**FEATURES OF ION EXCHANGE BETWEEN ELECTRODES IN METAL-ION ACCUMULATORS DURING DISCHARGE**

<sup>1</sup>*Institute of Geotechnical Mechanics named by N. Poljakov of National Academy of Sciences of Ukraine, Simferopolska St., 2, 49005, Dnipro, Ukraine; e-mail: Yeliseiev@nas.gov.ua*

<sup>2</sup>*Institute of Transport Systems and Technologies NAS of Ukraine Transmag, Piszarsky avenue 5, Dnipro, Ukraine;*

<sup>3</sup>*Oles Honchar Dnipro National University, Dnipro, Gagarin avenue 72, 49010, Dnipro, Ukraine;*

The importance and relevance of the storage of electrical energy is confirmed by events in the world and trends in the development and use of various electrical energy systems, household appliances, computer equipment, communication devices, etc. In addition to the growth of the metal-ion battery markets, there are trends towards a search for metals that in the future will be inexpensive and will have characteristics required for storage systems.

This paper considers ion exchange between the electrodes of metal-ion batteries whose charge carriers are metal ions, which diffuse in the process of discharge from the negative electrode to the positive one. A mathematical model was developed and tested. The model is based on a system of diffusion transport equations with the Nernst–Planck–Poisson potential equation replaced by an equivalent conductivity potential equation. Quasi-equilibrium regimes are considered.

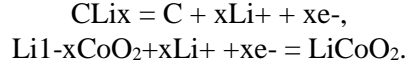
The entire working area consists of a pore electrode space and a neutral separator. The mathematical model employed consists of potential distribution equations and an electrolyte concentration distribution equation supplemented by the dependence of the electrode surface current on the overvoltage and equations that determine the electrode pore structure depending on the masses transferred inside the electrode.

The electric potential and diffuse component mass transfer equations are written within the framework of the modern theory of effective electrical conductivity in batteries with account for current exchange between the solid electrodes and the liquid electrolyte.

The research results showed the following. A change in the resistance of the separator (a change in porosity) has little effect, if any, on the electrode current densities, but it causes some change in the potentials themselves. A change in the resistance of the electrolyte affects both the electrode potentials and the internal current distribution between the electrodes and the electrolyte.

**Keywords:** *metal-ion battery, separator, anode, cathode, system of equations, porosity, potential, diffusion transport.*

**Introduction.** A feature of metal-ion batteries is that charge carriers in a liquid medium are metal ions such as Li, Na, K, Mg, Al, which, when discharged, leave the negative electrode in the form of positive ions, move to the positive one and intercalate into it [1, 2]. The electrochemical scheme of operation of such a battery using the example of lithium-ion can be written here, for example, in the form of the following reactions [3, 4]



The first reaction takes place on the negative electrode, the second - on the positive. It can be seen from the diagram that the amount of mass Li in the negative electrode determines the capacity of the battery, which decreases during discharge. When the battery is charged, the reactions go in the opposite direction, and the capacity returns, with the exception of losses, to its previous state. The mass content of the ion-forming metal in the electrode and in the electrolyte solution, of course, largely determines the magnitude of the voltage between the electrodes. The theory introduces the SOC value [5], which determines the relative capacitance of the electrodes. In our case, we will consider it a local value depending on the location of the point in the electrode.

Currently, there are two types of theories to describe the operation of batteries - these are applied, based on the theory of electrical circuits (equivalent circuits) [5, 6] and physical (electrochemical) theories based on the theory of ion exchange, for example [6, 7]. In this paper, we present a theoretical system developed in [8-10] and somewhat modified for metal-ion batteries. The entire area of the liquid accumulator can be schematically divided into three parts: the area of the negative electrode, the area of the positive electrode and the area between them occupied by the separator. The regions of the positive and negative electrodes consist of two different media - a porous solid with ohmic resistance and a liquid medium with almost diffusional ion transport.

Diffusion processes in solid electrodes [11] associated with the intercalation and deintercalation of the charge-carrying component are not considered. The use of the equations of diffusion transfer of ions in electrolytes, taking into account the Nernst-Planck-Poisson equation, encounters great mathematical difficulties [12], as a result of which simplifications are used in the battery theory associated with the replacement of the equation for the potential in the Nernst-Planck-Poisson form by the potential equation with equivalent conductivity.

**The purpose of the work** is a numerical analysis based on the known equations of the influence of certain parameters on ion exchange in batteries, as well as refinement of the mathematical model itself.

**Mathematical model.** Based on the developed theoretical provisions of works [8, 10], we write the basic equations in the following form, and we assume that the density of the electrolyte is considered constant:

$$\dagger_E \left( \frac{\partial^2 \xi_E}{\partial x^2} + \frac{\partial^2 \xi_E}{\partial y^2} \right) = j, \quad (1)$$

$$\dagger_R \left( \frac{\partial^2 \xi_R}{\partial x^2} + \frac{\partial^2 \xi_R}{\partial y^2} \right) = -j - \dagger_R \frac{RT}{F} \left( \frac{\partial^2 \ln f_{c_R}}{\partial x^2} + \frac{\partial^2 \ln f_{c_R}}{\partial y^2} \right), \quad (2)$$

$$\left( \frac{\partial \mathcal{V}_E c_E}{\partial t} + \frac{\partial \mathcal{V}_E u c_R}{\partial x} + \frac{\partial \mathcal{V}_E v c_R}{\partial r} \right) = \frac{j x m}{F \dots_R} + D_{REf} \left( \frac{\partial^2 c_R}{\partial x^2} + \frac{\partial^2 c_R}{\partial y^2} \right), \quad (3)$$

$$j = s j_0 \left[ \exp\left(\frac{r F}{R T} y\right) - \exp\left(-\frac{r F}{R T} y\right) \right], \quad (4)$$

$$\frac{\partial \dagger_E}{\partial t} = -\frac{j x m}{F \dots_E}, \quad \nu_E = 1 - \dagger_E. \quad (5)$$

The equation (1) determines the potential distribution in the solid part of the electrode (Ohm's law); equation (2) – potential distribution in the pore space of the electrode; equation (3) is the distribution of electrolyte concentrations in the pore space; the fourth expression establishes the dependence of the electric surface current of the electrode on the overvoltage; the fifth determines the pore structure of the electrode depending on the transferred masses inside the electrode.

The following notation is adopted in the equations:  $u, v$  – are electrolyte velocities;  $\epsilon$  – porosity;  $\{\}_E$  – is the potential at the electrode, V;  $\{\}_R$  – is the potential in the pore space of the electrode, V;  $F$  – is Faraday's constant, C/mol;  $c$  – is the mass concentration of the current-forming component;  $D_{Ref}$  – is the diffusion coefficient,  $\text{m}^2/\text{s}$ ;  $j_0$  – is the exchange current density,  $\text{A}/\text{m}^2$ ;  $s$  – is the specific surface area,  $1/\text{m}$ ;  $U$  – is the standard equilibrium potential between the electrode and the solution (for ion-metal batteries, this value depends on the capacitance of the electrodes);  $xm$  – is the value that establishes the relationship between the electric current and the transferred mass, kg/mol.

Taking into account that the electrodes are thin plates, the thickness of which is much less than other sizes, while the current is collected from the main wide area, the written equations can be rewritten in the form of one-dimensional equations:

$$\dagger_E^{-,+} \frac{\partial^2 \{\}_E^{-,+}}{\partial x^2} = j^{-,+}, \quad \dagger_E \frac{\partial^2 \{\}_E}{\partial x^2} = 0, \quad (6)$$

$$j^{-,+} = s^{-,+} j_0^{-,+} \left( \frac{c_R^{-,+}}{c_{R0}} \right)^n \dagger^{-,+} \left[ \exp\left(\frac{r F}{R T} y^{-,+}\right) - \exp\left(-\frac{r F}{R T} y^{-,+}\right) \right], \quad (7)$$

$$\frac{\partial c_E^{-,+}}{\partial t} = -\frac{j^{-,+} m}{F \dots^{-,+}}, \quad \dagger^{-} = \left( \frac{c_E^{-}}{c_{E0}^{-}} \right)^M, \quad \dagger^{+} = \left( 1 - \frac{c_E^{+}}{c_{E0}^{+}} \right)^P, \quad (8)$$

$$\dagger_R^{-,+} \frac{\partial^2 \{\}_R^{-,+}}{\partial x^2} = -j^{-,+} - \frac{R T}{F} \frac{\partial^2 \ln f c_R^{-,+}}{\partial x^2}, \quad (9)$$

$$\left( \frac{\partial V^{-,+} c_R^{-,+}}{\partial t} + \frac{\partial V^{-,+} u^{-,+} c_R^{-,+}}{\partial x} \right) = \frac{xm}{F_{\dots R}} j^{-,+} + D_{REF}^{-,+} \frac{\partial^2 c_R^{-,+}}{\partial x^2}, \quad (10)$$

$$\left( \frac{\partial v c_R}{\partial t} + \frac{\partial v u c_R}{\partial x} \right) = D_{REF} \frac{\partial^2 c_R}{\partial x^2}, \quad (11)$$

$$\frac{\partial V^{-,+}}{\partial t} = \frac{xm}{F_{\dots E}^{-,+}} j^{-,+}, \quad (12)$$

$$\left( \frac{\partial V^{-,+}}{\partial t} + \frac{\partial V^{-,+} u^{-,+}}{\partial x} \right) = \frac{xm}{F_{\dots R}} j^{-,+}, \quad (13)$$

where, the parameters with  $-$ ,  $+$  signs at the top refer to the corresponding electrodes, and without the index  $-$  to the separator.

With regard to system (1) – (5), these equations are supplemented with parameters  $\dagger^{-,+}$  [10] that play the role of local relative capacitances of electrodes ( $c_{E0}^{-,+}$  - are some limiting concentrations of ion-forming metal in electrodes,  $\dots_{E}^{-,+}$  - are electrode densities); reactions on the electrodes (intercolation on the positive and deintercolation on the negative). Let us now write out the boundary conditions. On the left border of the electrochemical cell (negative electrode axis):

$$\dagger_E^- \frac{\partial \xi_E^-}{\partial x} = i, \quad \frac{\partial \xi_R^-}{\partial x} = 0, \quad \frac{\partial c_R^-}{\partial x} = 0, \quad (14)$$

where:  $i$  is the current density at the current collector.

At the border of the negative electrode - separator:

$$\frac{\partial \xi_E^-}{\partial x} = 0, \quad \dagger_R^- \frac{\partial \xi_R^-}{\partial x} = \dagger_R \frac{\partial \xi_R}{\partial x}, \quad D_{REF}^- \frac{\partial c_R^-}{\partial x} = D_{REF} \frac{\partial c_R}{\partial x}. \quad (15)$$

At the separator-positive electrode boundary:

$$\frac{\partial \xi_E^+}{\partial x} = 0, \quad \dagger_R^+ \frac{\partial \xi_R^+}{\partial x} = \dagger_R \frac{\partial \xi_R}{\partial x}, \quad D_{REF}^+ \frac{\partial c_R^+}{\partial x} = D_{REF} \frac{\partial c_R}{\partial x}. \quad (16)$$

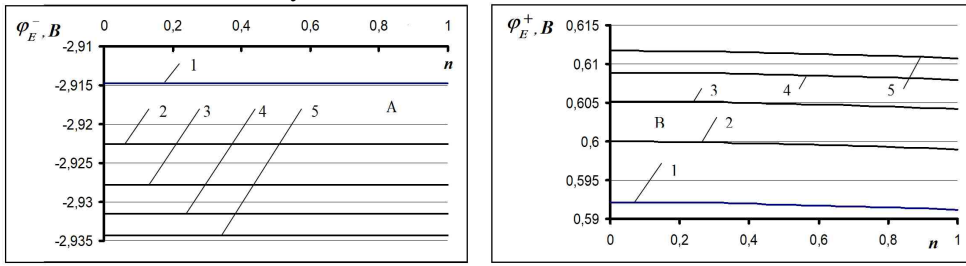
On the right border of the electrochemical cell (positive electrode axis):

$$\dagger_E^+ \frac{\partial \xi_E^+}{\partial x} = -i, \quad \frac{\partial \xi_R^+}{\partial x} = 0, \quad \frac{\partial c_R^+}{\partial x} = 0. \quad (17)$$

**Results of calculations and their discussion.** The results presented here are of a qualitative nature, due to the fact that the parameters underlying the calculations, taken from literary sources, such as [7–9, 13, 14], are not tied to specific devices, but are used in the form of some approximate values. Numerical calculations are based on an explicit numerical scheme, which is convenient for counting control and has proven itself in such problems [10, 12]. The calculation results are shown in Figs. 1 – 4. The main issue that was put before this study is to determine the influence of some basic parameters (electrical resistance of the medium, over-

voltage) on the distribution of potentials and current densities in the electrodes and separator.

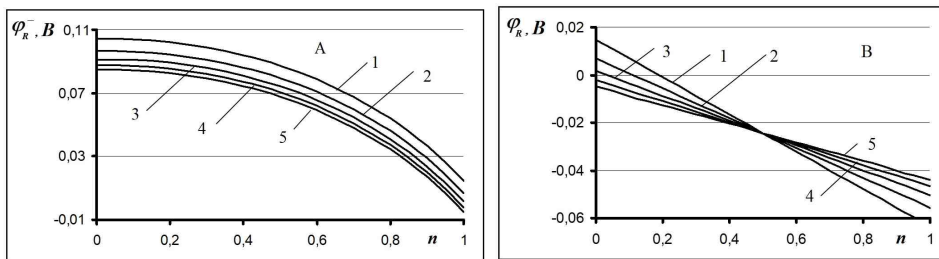
On fig. 1 and 2 show the potential distributions in the electrodes and electrolyte for the case when the resistance of the separator changes due to its porosity at a constant current density set in the current collector.



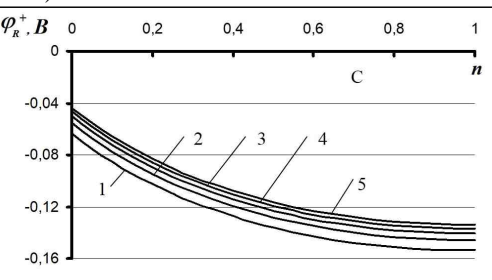
a) – negative electrode; b) is positive

1 –  $\epsilon = 0,4$ ; 2 –  $0,5$ ; 3 –  $0,6$ ; 4 –  $0,7$ ; 5 –  $0,8$ .

Fig. 1 – Potential distribution in electrodes



a) – negative electrode; b) – separator; c) – positive electrode



c)

1 –  $\epsilon = 0,4$ ; 2 –  $0,5$ ; 3 –  $0,6$ ; 4 –  $0,7$ ; 5 –  $0,8$ .

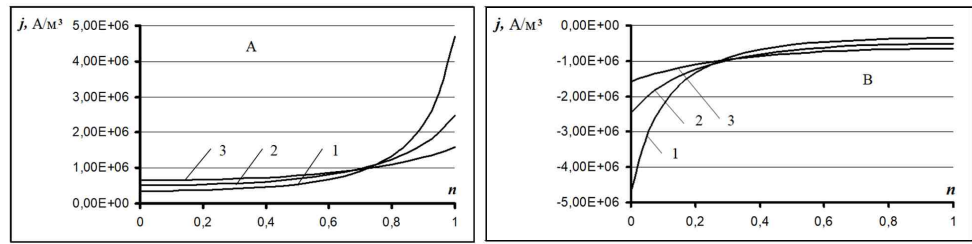
Fig. 2 – Potential distribution in pore spaces

The following values were taken in the calculations:

- plate thicknesses  $h^- = h^+ = 3$  mm,  $h = 1$  mm;
- electrode porosity  $\epsilon^- = \epsilon^+ = 0,4$ ;
- conductivity  $\sigma^- = 4,8 \cdot 10^5$  ( $1 - \epsilon^-$ ) S/m;  $\sigma^+ = 8000$  ( $1 - \epsilon^+$ ) S/m;
- $R = R_0$ ,  $R_0 = 80$  S/m (conductivity of the electrolyte);
- standard equilibrium potentials  $U^- = -3,29$  V,  $U^+ = 0,91$  V,  $\gamma^+ = 1$ .

It follows from these figures that an increase in the conductivity of the separator (increase in porosity) leads to a slight increase in the absolute value of the potentials in the solid part of the electrodes, but to a decrease in the potentials in the corresponding pore spaces. However, these variations in the electrical resistance of the separator do not lead to a change in the current densities in the electrodes.

Figure 3 shows the distribution curves of the current densities, of which the number 2 shows the curves corresponding to the above series of calculations, i.e. changes in the electrical resistance of the separator practically do not change the distribution of current densities in the electrodes.

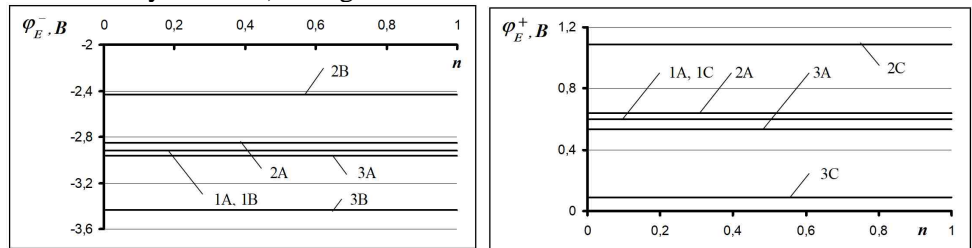


a) negative electrode; b) positive electrode.  
1 –  $R_0 = 40 \text{ S/m}$ ; 2 –  $80 \text{ S/m}$ ; 3 –  $160 \text{ S/m}$ .

Fig. 3 – Current density in electrodes

However, if the electrical conductivity of the electrolyte is changed, then, as can be seen from Fig. 3 according to curves 1, 3, this noticeably affects the density distribution. In this case, a decrease in the conductivity of the electrolyte leads to a greater inhomogeneity of the distribution. In current collectors (in fig. a) - on the left; in fig. b) - on the right), the densities slightly decrease in absolute value, and at the opposite ends of the electrodes, the values increase sharply.

A change in the conductivity of electrolytes affects not only the distributions of current densities, but also the distributions of potentials in both electrodes, as evidenced by curves a) in Fig. 4.



a) negative electrode,

– change in the electrical conductivity of the electrolyte:

1A –  $R_0 = 80 \text{ S/m}$ ; 2A –  $40 \text{ S/m}$ ; 3A –  $160 \text{ S/m}$ ;

– change in overvoltage:

1B –  $U^- = -3,29 \text{ V}$ ,  $U^+ = 0,91 \text{ V}$ ; 2B –  $U^- = -2,8 \text{ V}$ ; 3B –  $U^- = -3,8 \text{ V}$ .

b) positive electrode,

– change in the electrical conductivity of the electrolyte:

1A –  $R_0 = 80 \text{ S/m}$ ; 2A –  $40 \text{ S/m}$ ; 3A –  $160 \text{ S/m}$ ;

– change in overvoltage:

1C –  $U^- = -3,29 \text{ V}$ ,  $U^+ = 0,91 \text{ V}$ ; 2C –  $U^+ = 1,4 \text{ V}$ ; 3C –  $U^+ = 0,4 \text{ V}$ .

Fig. 4 – Potential distribution in the electrodes

It follows from it that a decrease in the electrical conductivity of electrolytes leads to a certain decrease in the absolute value of the potentials of the electrodes. Curves b) in fig. 4 A and curves c) in Fig. 4 b) show the effect of changing the standard potentials, from which it follows that an increase in the absolute value of  $U$  leads to an increase in the potential of this electrode, respectively. All other parameters change only slightly. Thus, the calculations showed that the electrical

conductivity of the electrolyte has a significant effect on the distribution of parameters. To some extent, this indirectly confirms the conclusions made in [15] about the role of electrolyte in electrochemical transformations.

**Conclusions.** As a result of the theoretical studies carried out, the following results were obtained:

1) the calculations performed showed that a change in the resistance of the separator (change in porosity) leads to some change in the potentials in the electrodes and in their pore spaces, but practically does not change the distribution of current densities;

2) change in the electrolyte resistance affects both the magnitude of the potentials in the electrodes and the distribution of internal currents between the electrodes and the electrolyte.

1. Verma J., Kumar D. Metal-ion batteries for electric vehicles: current state of the technology, issues and future perspective. *Nanoscale Adv.* 2021. V. 3, No. 12. P. 3384. <https://doi.org/10.1039/D1NA00214G>
2. Koshel M. D. Theoretical Foundations of Electrochemical Energetics. Dnipropetrovsk: UDKhTU, 2002. 430 p. (in Ukrainian).
3. Byk M. V., Frolenkova S. V., Buket O. I., Vasylev H. S. Engineering Electrochemistry. Part 2. Chemical Current Sources. Kyiv: KPI, 2018. 321 p. (in Ukrainian).
4. Ramos A. M. On the well-posedness of a mathematical model for lithium-ion batteries *Applied Mathematical Modelling*. 2016. V. 40. P. 115–125. <https://doi.org/10.1016/j.apm.2015.05.006>
5. Binelo M. F. B., Sausen A. T. Z. R., Sausen P. S., Binelo M. O. Mathematical modeling and parameter estimation of battery lifetime using a combined electrical model and a genetic algorithm. *Tend. Mat. Apl. Comput.* 2019. V. 20, No. 1. P. 150–167. <https://doi.org/10.5540/tema.2019.020.01.149>
6. Borakhadikar Ashwin S. One Dimensional Computer Modeling of a Lithium-Ion Battery A thesis submitted in partial fulfillment of the requirements for the degree of Master of Science in Mechanical Engineering. Shivaji University, Kolhapur, 2013. 71 p.
7. Esfahanian Vahid, Torabi Farschad, Mosahebi Ali . An improved mathematical model of lead-acid batteries for simulation of VRLA batteries. *Journal of Power Sources Symposium*. 2007. 9 p. URL: <https://wp.kntu.ac.ir/ftorabi/Resources/Publications/An%20Improved%20Mathematical%20Model%20of%20Lead%20acid%20E2%80%93Acid%20Batteries%20for%20Simulation%20of%20VRLA%20Batteries.pdf> (Last accessed on April 28, 2023).
8. Esfahanian Vahid, Kheirhan Pooyan, Bahramian Hassan, Ansori Amir Babac, Ahmadi Goodarz. The effects of electrode parameters on lead-acid battery performance. *Advanced Materials Research*. 2013. V. 651. P. 492–498. <https://doi.org/10.4028/www.scientific.net/AMR.651.492>
9. Gu Hiram, Nguyen T. V., White R. E. A mathematical model of a lead-acid cell: discharge, rest, and charge. *J. Electrochem. Soc. Electrochemical Science and Technology*. 1987. V. 134, No. 12. P. 2953–2960. <https://doi.org/10.1149/1.2100322>
10. Yeliseyev V. I., Sovit Yu. Change in the potential of a liquid battery on external circuit closing. *Bulletin of Dnipro University. Series: Mechanics*. 2021. V.29, No 6. Is. 25. P. 54–65. (in Ukrainian).
11. Yi Zeng. Mathematical Modeling of Lithium-Ion Intercalation Particles and Their Electrochemical Dynamics. Ph.D. Thesis. Massachusetts Institute of Technology, 2015. . 190. <https://dspace.mit.edu/handle/1721.1/99062> (Last accessed on April 28, 2023)
12. Yeliseyev V. I., Sovit Yu. P., Bliuss B. A. Ion transfer in convective/diffusion flow separation. In: *Aerospace Hardware System Design and Performance Analysis*. V. XXVI. Dnipro, 2019. P. 21–38. (in Ukrainian). <https://doi.org/10.15421/471904>
13. Shah A.A., Li X., Wills R.G.A., Walsh F.C. A mathematical model for the soluble lead-acid flow battery. *J. of the Electrochemical Society*. 2010. V. 157. No. 5. P. A589–A599. <https://doi.org/10.1149/1.3328520>
14. Beneš M., Fuř R., Havlena V., Klement V., Kolář M., Polívka O., Solovský J, Strachota P. An efficient and robust numerical solution of the full-order multiscale model of lithium-ion battery. *Mathematical Problems in Engineering*. 2018. Article ID 3530975. <https://doi.org/10.1155/2018/3530975>
15. Apostolova R. D., Zadorei N. D., Kolomoets O. V., Shembel E. M. Comparative assessment of electrochemical sulfides' electrochemical conversion efficiency in a prototype lithium battery depending on the nature of the liquid electrolyte. *Voprosy Khimii i Khimicheskoi Tekhnologii*. 2012. No. 2. P. 186–190. (in Russian). URL: <https://udhtu.edu.ua/public/userfiles/file/VHHT/2012/2/%D0%90postolova.pdf> (Last accessed on April 28, 2023).

Received on July 20, 2023,  
in final form on September 18, 2023